

Magnetic excitations in the spin- $\frac{5}{2}$ antiferromagnetic trimer substance SrMn₃P₄O₁₄Masashi Hase,^{1,*} Masaaki Matsuda,^{2,3} Koji Kaneko,² Naoto Metoki,² Kazuhisa Kakurai,² Tao Yang,⁴ Rihong Cong,⁴ Jianhua Lin,⁴ Kiyoshi Ozawa,¹ and Hideaki Kitazawa¹¹*National Institute for Materials Science, 1-2-1 Sengen, Tsukuba, Ibaraki 305-0047, Japan*²*Japan Atomic Energy Agency, 2-4 Shirakata Shirane, Tokai, Naka, Ibaraki 319-1195, Japan*³*Oak Ridge National Laboratory, Oak Ridge, Tennessee 37831, USA*⁴*College of Chemistry and Molecular Engineering, Peking University, Beijing 100871, People's Republic of China*

(Received 6 June 2011; revised manuscript received 11 November 2011; published 2 December 2011)

A quantum-mechanical $1/3$ magnetization plateau and magnetic long-range order appear in the large-spin ($5/2$) substance SrMn₃P₄O₁₄. Previous magnetization results suggest that the spin system consists of antiferromagnetic trimers that are weakly coupled with one another. We inferred that the magnetization plateau originated from discrete energy levels of the trimer. In order to confirm the discrete energy levels, we performed inelastic neutron-scattering experiments on SrMn₃P₄O₁₄ powders. Observed magnetic excitations are consistent with excitations expected in the trimer model.

DOI: [10.1103/PhysRevB.84.214402](https://doi.org/10.1103/PhysRevB.84.214402)

PACS number(s): 75.40.Gb, 75.10.Jm, 75.47.Lx, 75.50.Ee

I. INTRODUCTION

A quantum-mechanical nature is sometimes apparent even in an ordered state of several low-dimensional spin systems formed by small spins. In the triangular antiferromagnet CsCuCl₃ with spin $1/2$, a small jump was observed in the magnetization curve in the magnetic field parallel to the c axis.¹ This jump was successfully explained as a spin-flop process caused by quantum-mechanical effects.² In spin-gap systems with spin $1/2$ such as the spin-Peierls system in CuGeO₃^{3,4} and the two-leg ladder system in SrCu₂O₃,^{5,6} antiferromagnetic (AF) long-range order (LRO) appears when small amounts of impurities were doped.⁷⁻¹¹ Nonetheless excitations originating in the singlet-triplet gap in the pure system were observed.¹² In the spin-tetramer substance Cu₂CdB₂O₆ with spin $1/2$, a quantum-mechanical $1/2$ magnetization plateau exists in the ordered state.^{13,14}

A quantum-mechanical nature can be seen in some spin systems formed by large spins. The famous examples are single-molecule magnets such as [Mn₁₂(CH₃COO)₁₆(H₂O)₄O₁₂] \cdot 2CH₃COOH \cdot 4H₂O.¹⁵⁻¹⁷ Macroscopic quantum tunneling of the magnetization was observed. Another example is the spin- $5/2$ substance SrMn₃P₄O₁₄, which shows a quantum-mechanical $1/3$ magnetization plateau.¹⁸ The magnetization plateau can remain even in the ordered state. The magnetization plateau cannot be understood in a classical picture (arrangement of ordered magnetic moments). In order to investigate the origin of the magnetization plateau, we measured magnetizations in the magnetic field up to 58 T.¹⁹ We could explain the magnetic field, H , and temperature, T , dependences of the magnetization using the spin- $5/2$ trimer formed by the AF J_1 interaction ($J_1 = 4.0$ K) depicted as ellipses in Fig. 1. The spin trimer has discrete energy levels in a quantum-mechanical picture. The magnetization in the magnetic fields of the plateau (2–10 T) cannot increase with increasing field because of an energy gap between the plateau state (total spin $5/2$) and the higher state (total spin $7/2$).¹⁹

In order to confirm the discrete energy levels of the AF trimer, we performed inelastic neutron scattering (INS) experiments on SrMn₃P₄O₁₄ powders. We expected magnetic

excitations with weak dispersion that could be observed in constant- Q (magnitude of the scattering vector) scan spectra and information on the Mn-Mn distance of the strongest exchange interaction from constant- ω (energy transfer) scan spectra.²⁰⁻²²

II. METHODS OF EXPERIMENTS

We synthesized single crystals of SrMn₃P₄O₁₄ under hydrothermal conditions at 473 K.¹⁸ Each crystal was small. We used pulverized crystals for INS measurements.

We carried out INS measurements on the cold-neutron triple-axis spectrometer LTAS installed at JRR-3M at the Japan Atomic Energy Agency (JAEA). The final neutron energy was fixed at 2.6 meV. Higher-order beam contamination was effectively eliminated using a cooled Be filter before the sample. The horizontal collimator sequence was guide-80°-Be-sample-120°-open. This setup yields an energy resolution of 0.1 meV (full width at half maximum, FWHM) at an energy transfer $\omega = 0$ meV. The resolution was determined from incoherent scattering of the sample. A powder sample of about 9 g was mounted in a ⁴He closed-cycle refrigerator.

III. RESULTS AND DISCUSSION

We performed all the INS measurements above the transition temperature. Circles in Fig. 2 show the ω dependence of the INS intensity (constant- Q scan spectra) around 5 K. The value of Q is the magnitude of the scattering vector. Excitations are apparent between 0.5 and 1.5 meV. Two kinds of excitations with different peak positions seem to overlap each other. The spectra are almost independent of Q except for differences in intensities. The weak Q dependence indicates that the excitations are transitions between discrete energy levels. We consider that the intensities in the vicinity of 0 meV cannot be explained only by incoherent scattering because of the T dependence of the spectra, as shown later. Low-energy excitations exist.

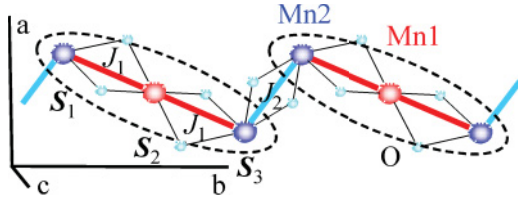


FIG. 1. (Color online) A schematic drawing of the positions of Mn^{2+} ions ($3d^5$) having localized spin $5/2$ in $\text{SrMn}_3\text{P}_4\text{O}_{14}$.¹⁸ Two crystallographically independent Mn^{2+} sites (Mn1 and Mn2) exist. Two kinds of short Mn-Mn bonds exist and have Mn-O-Mn paths. The Mn-Mn distances are 3.27 and 3.34 Å at room temperature. The exchange interaction parameters are respectively defined as J_1 and J_2 . The dominant AF J_1 interactions form the spin trimers indicated by the ellipses. The Hamiltonian is expressed as $\mathcal{H} = J_1(S_1S_2 + S_2S_3)$. The spin trimer can account for the magnetic field and temperature dependences of the magnetization when $J_1 = 4.0$ K. Mn-Mn distances in the other bonds are more than 4.89 Å. These bonds have no Mn-O-Mn paths.

We compared each spectrum above 0.2 meV in Fig. 2 with a sum of two Gaussians and one Lorentzian (plus constant backgrounds).

$$I(\omega) = \frac{I_0 a_0}{\pi} \frac{1}{\omega^2 + a_0^2} + \sum_i \frac{I_i}{\sqrt{\pi} a_i} \exp\left[-\frac{(\omega - \omega_i)^2}{a_i^2}\right] + I_{\text{BG}}. \quad (1)$$

Here the sum is from $i = 1-2$. The two Gaussians correspond to the excitations between 0.5 and 1.5 meV. The Lorentzian corresponds to the excitations in the vicinity of 0 meV. Each sum of two Gaussians and one Lorentzian (solid line)

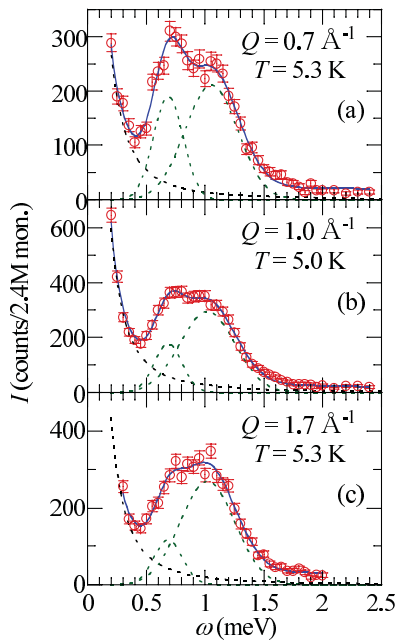


FIG. 2. (Color online) The inelastic neutron-scattering intensity vs energy transfer ω [constant- Q (magnitude of the scattering vector) scan spectra] of $\text{SrMn}_3\text{P}_4\text{O}_{14}$ around 5 K (circles). The solid line represents the sum of two Gaussians and one Lorentzian (plus constant backgrounds). The dashed lines indicate each Gaussian or Lorentzian. The values of the parameters are given in Table I.

reproduces well the corresponding spectrum in Fig. 2. The obtained values of the fitting parameters are shown in Table I. The peak position in the spectrum at $Q = 1.0 \text{ \AA}^{-1}$ is 0.68 meV or 1.02 meV. The peak width (FWHM) is 0.28 and 0.55 meV for the 0.68 and 1.02 meV excitations, respectively. These widths are larger than the energy resolution of 0.1 meV at $\omega = 0$ meV, indicating the existence of weak dispersion caused by intertrimer interactions.

The circles in Fig. 3 show constant- Q scan spectra at $Q = 1.0 \text{ \AA}^{-1}$. The 0.68- and 1.02-meV excitations are also seen at 11.2 K. Intensities around 0.5 meV are larger at 11.2 K than at 5.0 K, suggesting the appearance of another transition. Therefore, we compared the spectrum above 0.2 meV at 11.2 K with a sum of three Gaussians and one Lorentzian (plus constant backgrounds), given in Eq. (1) with $i = 1-3$. To reduce variable parameters, we assumed that the peak position (0 meV) of the Lorentzian and the peak positions (0.68 and 1.02 meV) and widths of the two Gaussians were constant. We used the values obtained at 5.0 K. This assumption is reasonable for transitions between discrete energy levels. The sum of the three Gaussians and one Lorentzian (solid line) reproduces well the spectrum at 11.2 K. The peak position of the third Gaussian is 0.46 meV. The peak width (FWHM) is 0.25 meV and is larger than the energy resolution of 0.1 meV at $\omega = 0$ meV.

The spectra at 15.6 and 20.3 K shown, respectively, in Figs. 3(b) and 3(c) resemble the spectrum at 11.2 K. Therefore, we compared the spectrum above 0.2 meV at 15.6 K or 20.3 K with a sum of three Gaussians and one Lorentzian (plus constant backgrounds), given in Eq. (1) with $i = 1-3$. In the fitting, we assumed that the peak position of the Lorentzian and the peak positions and widths of the three Gaussians were constant. The sum (solid line) reproduces well each experimental spectrum. Spectra are featureless above 30 K. We did not compare the spectra with calculated curves. The integrated intensity between 0.5 and 1.5 meV decreases slightly on heating. The Bose factor proportional to phonon intensity at 0.68 meV and 20.3 K, on the other hand, is about 9 times as large as that at 0.68 meV and 5.0 K. Therefore, the contribution of the phonon is small enough, and magnetic excitations are dominant between 0.5 and 1.5 meV.

We examined whether the spin- $5/2$ AF trimer model with $J_1 = 4.0$ K can account for the observed excitations. Figure 4(a) depicts a schematic drawing of low-lying energy levels.¹⁹ The following selection rules of transitions are derived theoretically.²³

$$\Delta S = 0, \pm 1, \quad \Delta M = 0, \pm 1, \quad \Delta S_{13} = 0, \pm 1. \quad (2)$$

S_i ($i = 1, 2, 3$) is the spin operator in the trimer. S and S_{13} are defined as $S_1 + S_2 + S_3$ and $S_1 + S_3$, respectively. M is the z component of S . Arrows in Fig. 4(a) indicate allowed transitions from the ground state (GS), first excited state (IES), or second excited states (2ES). In our experimental setup, we can observe transitions with an energy difference $\Delta\epsilon$ up to 8 when $J_1 = 4.0$ K. Here ϵ is defined as E/J_1 (E is eigenenergy).

Figure 4(b) depicts the T dependence of the calculated occupation ratio of the five low-lying energy levels. An inelastic neutron-scattering intensity strongly depends on the occupation ratio. From Fig. 4(b), we know that excitations

TABLE I. Values of the integrated intensity I_i and FWHM of a Lorentzian or Gaussian obtained from fitting Eq. (1) to the experimental constant- Q spectra of $\text{SrMn}_3\text{P}_4\text{O}_{14}$. FWHM is given as $2a_0$ for the Lorentzian and $2\sqrt{\ln 2}a_i$ for the Gaussian. In fitting to the spectra at $Q = 1.0 \text{ \AA}^{-1}$, the value of FWHM of each Gaussian was obtained at 5.0 or 11.2 K and was fixed in the fitting at higher T . The values in parentheses indicate errors.

Q (\AA^{-1})	T (K)	0 meV		0.68(1) meV		1.02(2) meV		0.46(5) meV	
		I_0	FWHM (meV)	I_1	FWHM (meV)	I_2	FWHM (meV)	I_3	FWHM (meV)
0.7	5.3	379(58)	0.24(8)	60(9)	0.30(3)	119(11)	0.53(5)		
0.8	5.7	475(136)	0.31(10)	58(8)	0.34(4)	159(21)	0.62(10)		
1.0	5.0	1091(33)	0.16(4)	52(9)	0.28(3)	172(13)	0.55(4)		
1.2	5.4	1123(34)	0.16(4)	32(9)	0.25(5)	190(14)	0.53(4)		
1.5	5.1	968(54)	0.18(3)	31(6)	0.23(3)	177(13)	0.54(3)		
1.7	5.3	795(51)	0.16(4)	36(13)	0.29(6)	157(13)	0.55(6)		
1.0	5.0	1091(33)	0.16(4)	52(9)	0.28(3)	172(13)	0.55(4)		
	11.2	562(296)	0.43(20)	36(6)	0.28	156(12)	0.55	17(12)	0.25(0.14)
	15.6	515(78)	0.53(7)	31(6)	0.28	141(12)	0.55	17(11)	0.25
	20.3	518(179)	0.56(16)	29(6)	0.28	117(11)	0.55	17(10)	0.25

from GS are dominant around 5 K. We considered that the 0.68- and 1.02-meV excitations correspond to transitions from GS to 1ES and 2ES, respectively, indicated by black arrows. The respective energy differences are $2.5J_1$ and $3.5J_1$. The value of J_1 is evaluated as 0.27 meV (3.2 K) or 0.29 meV (3.4 K). These values are slightly smaller than the value determined in the magnetization results ($J_1 = 4.0$ K). Excitations from 1ES or 2ES are also expected at 11.2 K. We considered that the 0.46-meV excitation corresponds to the transition from 2ES to 4ES, indicated by a black arrow. The energy difference is $1.5J_1$. The value of J_1 is evaluated as 0.30 meV

(3.5 K) and is close to the values evaluated from the other two transitions.

We examined whether we observed all the allowed transitions that are possible in our experimental setup. As was described, we observed the three black arrow transitions. The gray arrow transitions may exist. However, we could not prove the existence of the gray arrow transitions. Energy differences of some gray arrow transitions ($2.5J_1$ and $4J_1$) are the same as or close to the energy differences of black arrow transitions ($2.5J_1$ and $3.5J_1$). Therefore, we could not extract the contribution of the gray arrow transitions from the exper-

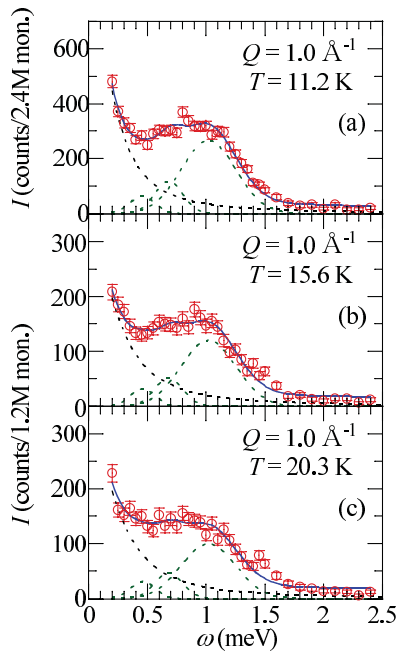


FIG. 3. (Color online) Constant- Q scan spectra of $\text{SrMn}_3\text{P}_4\text{O}_{14}$ at $Q = 1.0 \text{ \AA}^{-1}$ (circles). The solid line represents the sum of three Gaussians and one Lorentzian (plus constant backgrounds). The dashed lines indicate each Gaussian or Lorentzian. The values of the parameters are given in Table I.

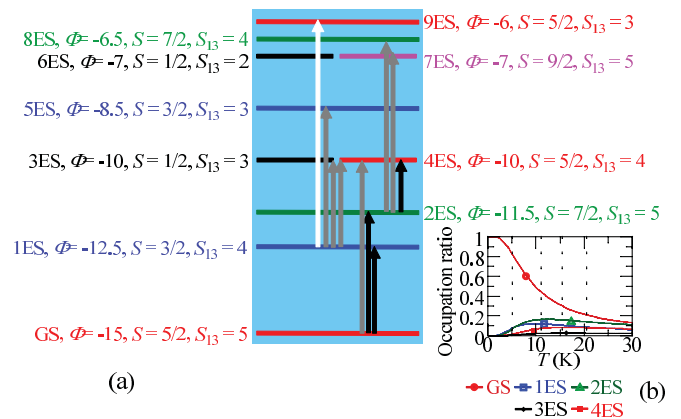


FIG. 4. (Color online) (a) A schematic drawing of low-lying energy levels in the spin- $5/2$ AF linear trimer [ground state (GS) and excited states (ESs)].¹⁹ The parameters $\epsilon \equiv E/J_1$ and S indicate the eigenenergy and the total spin, respectively. S_{13} is defined in the text. To distinguish two degenerate eigenstates with $\epsilon = -10$, we name the two states 3ES and 4ES. To distinguish two degenerate eigenstates with $\epsilon = -7$, we name the two states 6ES and 7ES. The arrows indicate allowed transitions from GS, 1ES, or 2ES with an energy difference $\Delta\epsilon$ up to 8. We observed the three black arrow transitions. The gray arrow transitions may exist. We could not detect the white arrow transition. (b) The temperature dependence of the calculated occupation ratio of the five low-lying energy levels when $J_1 = 4.0$ K.

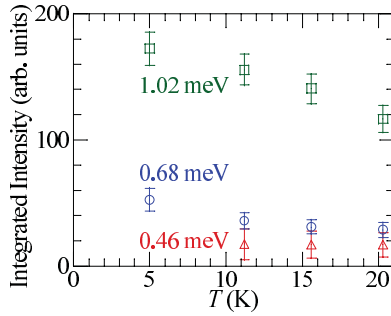


FIG. 5. (Color online) The temperature dependence of the integrated intensity of the 0.46-, 0.68-, and 1.02-meV excitations in $\text{SrMn}_3\text{P}_4\text{O}_{14}$ at $Q = 1.0 \text{ \AA}^{-1}$.

imental results. Energy differences of the other gray arrow transitions are $4.5J_1 = 1.3 \text{ meV}$ and $5J_1 = 1.4 \text{ meV}$ when $J_1 = 0.29 \text{ meV}$. Small INS intensities are seen around these energies in Figs. 2 and 3. In our analyses, the small intensities correspond to the tail of the 1.02-meV excitation. However, the peak width is larger in the 1.02-meV excitation (FWHM = 0.55 meV) than in the 0.46-meV excitation (FWHM = 0.25 meV) or the 0.68-meV excitation (FWHM = 0.28 meV). The gray arrow transitions may exist in the tail. We could not detect the white arrow transition. We do not have theoretical INS intensities. Therefore, we could not determine the reason why we could not detect the white arrow transition. The INS intensity of the white arrow transition may be very small. Transitions from 3ES or higher excited states must exist at 11.2 K and higher T . However, we could not prove the existence of these transitions because of the same reason as for the gray arrow and white arrow transitions in Fig. 4(a).

Figure 5 shows the T dependence of the integrated intensity of the 0.46-, 0.68-, and 1.02-meV excitations. The integrated intensity of the 0.46-meV excitation is nearly independent of T . The integrated intensity of the 0.68- or 1.02-meV excitation gradually decreases with increasing T . As is shown in Fig. 4(a), several transitions are expected to exist. Therefore, the T dependence of the integrated intensity in Fig. 5 cannot be compared directly with the occupation ratios in Fig. 4(b).

The Q dependence of the INS intensity in the AF trimer is given in the following formula:^{23–25}

$$I(Q) = A_1 f(Q)^2 [1 - \sin(3.27Q)/(3.27Q)] + A_2 f(Q)^2 [1 - \sin(6.54Q)/(6.54Q)]. \quad (3)$$

The values 3.27 and 6.54 indicate the Mn1-Mn2 and Mn2-Mn2 lengths in the AF trimer, respectively. The function $f(Q)$ is the magnetic form factor of Mn^{2+} ions.²⁶ The coefficients A_1 and A_2 depend on two eigenstates between which the transition occurs. The coefficients are not derived theoretically. Figure 6(a) represents the two terms in Eq. (3). Circles in Figs. 6(b)–6(d) show constant- ω scan spectra of $\text{SrMn}_3\text{P}_4\text{O}_{14}$. The lines indicate the first term in Eq. (3) plus constant backgrounds. The INS intensity in the vicinity of $\omega = 2 \text{ meV}$ is small and almost independent of ω , Q , and T . Therefore, we used the intensity at $\omega = 2 \text{ meV}$ for the value of constant backgrounds. Each line is consistent with the corresponding constant- ω scan spectrum. If A_1 is much larger than A_2 in

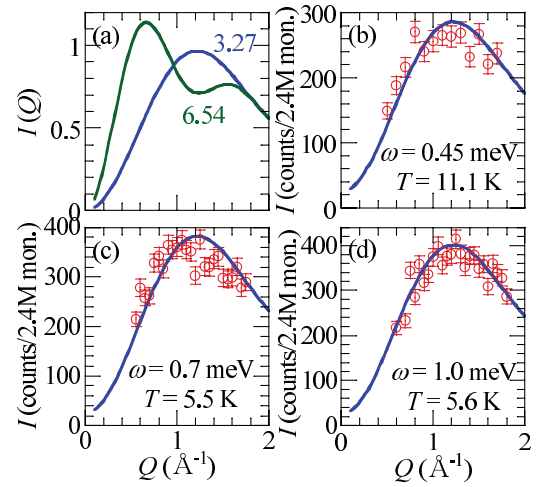


FIG. 6. (Color online) (a) The Q dependence of the calculated INS intensity in the spin-5/2 AF linear trimer. (b)–(d) The inelastic neutron-scattering intensity vs Q (constant- ω scan spectra) of $\text{SrMn}_3\text{P}_4\text{O}_{14}$ (circles). The line indicates the first term in Eq. (3).

the observed transitions, this consistency indicates that the AF trimer model can explain the experimental $I(Q)$.

We comment on intertrimer interactions. The dispersion relation of magnetic excitations was calculated in spin dimers with weak interdimer interactions using random phase approximation.²⁷ A similar dispersion relation was inferred in interacting spin tetramers.²⁸ According to the results, we speculate that the following dispersion relation may be applicable to spin trimers with weak intertrimer interactions:

$$\omega_{\mathbf{q}=(h,k,l)} = \sqrt{\Delta^2 + \alpha \Delta J(\mathbf{q}) R(T)}. \quad (4)$$

Here Δ is an energy difference between ground and excited states, and α is a coefficient derived from transition matrix elements. The value of α is 2 for the spin-1/2 dimer²⁹ or 5 for the spin-3/2 dimer.²⁷ $J(\mathbf{q})$ is a Fourier transform of intertrimer interactions. $R(T)$ is the difference in the thermal populations of ground and excited states. We consider that the dominant intertrimer interaction is the J_2 interaction. $J(\mathbf{q})$ is expressed approximately as $2J_2 \cos(2\pi k)$. We assume that excitation energies are the same at 0 and 5.0 K. The excitation energy at 0 K at the bottom of the dispersion ω_b , where the INS intensity is the strongest, is expressed as follows:

$$\omega_b = \sqrt{\Delta^2 - 2\alpha \Delta J_2}. \quad (5)$$

We assume that only the J_2 interaction is the origin of the difference between the expected excitation energy $2.5J_1 = 10 \text{ K}$ and the experimental excitation energy $0.68 \text{ meV} = 7.9 \text{ K}$ in the transition between GS and 1ES. Using $\Delta = 10 \text{ K}$ and $\omega_b = 7.9 \text{ K}$, we obtained $\alpha J_2 = 1.9 \text{ K}$. If α is large, a J_2 value can be small enough in comparison with the J_1 value.

We observed magnetic excitations that are consistent with excitations expected in the spin-5/2 AF trimer. Therefore, the discrete energy levels of the AF trimer are the origins of the quantum-mechanical nature (magnetization plateau) in $\text{SrMn}_3\text{P}_4\text{O}_{14}$. In the strict sense, the energy difference between GS ($S = 5/2$) and 2ES ($S = 7/2$) generates the magnetization plateau. The magnetization plateau appears

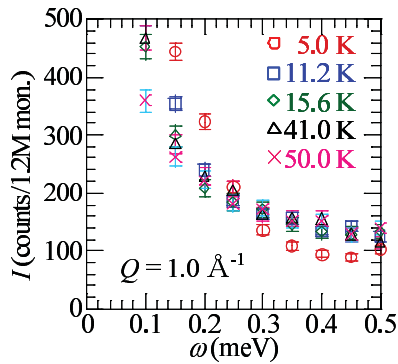


FIG. 7. (Color online) Constant- Q scan spectra of $\text{SrMn}_3\text{P}_4\text{O}_{14}$ at $Q = 1.0 \text{ \AA}^{-1}$.

even in the ordered state.^{18,19} The property of the cluster (trimer in this case) can remain in the ordered state. The total spin of the ground state of the AF trimer is finite ($5/2$). Therefore, we consider that the magnetic LRO is stabilized by the J_1 and weak three-dimensional intertrimer interactions. Several cluster substances can maintain their cluster properties in their ordered states. For example, the $1/2$ quantum-mechanical magnetization plateau is generated by discrete energy levels of a spin- $1/2$ tetramer in $\text{Cu}_2\text{CdB}_2\text{O}_6$.^{13,14} The plateau remains in the ordered state. With the aid of other researchers, some of the present authors determined the magnetic structure below the transition temperature of $T_N = 2.2(1) \text{ K}$ using neutron-powder-diffraction data.³⁰ The magnetic structure has a long-range period. We are now considering the origin of the long-range period. We will report the details of the magnetic structure in a subsequent presentation.

We comment on the INS intensity in the vicinity of 0 meV . Figure 7 shows constant- Q scan spectra at $Q = 1.0 \text{ \AA}^{-1}$ below 0.5 meV . As was described, the increase of the intensity around 0.4 meV is caused by the 0.46-meV excitation. The intensity between 0.1 and 0.2 meV decreases with increasing T . This temperature dependence cannot be explained by incoherent scattering or phonons. In addition, we observed diffuse scattering between $2\theta = 15$ and 40° in neutron-powder-diffraction patterns (wavelength $\lambda = 2.458 \text{ \AA}$).³⁰ This

2θ range corresponds to $Q = 0.7\text{--}1.7 \text{ \AA}^{-1}$ in the present INS experiments. The shape of the diffuse scattering resembles one-dimensional or two-dimensional Bragg scattering with a cutoff at low Q and a long tail at large Q . The integrated intensity of the diffuse scattering shows a maximum in the vicinity of T_N . Several magnetic reflections appear below T_N between $2\theta = 15^\circ$ and 40° . Therefore, the origin of the diffuse scattering is magnetic. Consequently, magnetic excitations exist in the vicinity of 0 meV . The magnetic excitations cannot be explained by transitions between energy levels in the trimer. Spin fluctuation in the ground state generates the magnetic excitations. Therefore, we used the Lorentzian with the 0-meV peak in fitting the constant- Q scan spectra in Figs. 2 and 3. In future studies, we will perform INS measurements of $\text{SrMn}_3\text{P}_4\text{O}_{14}$ in the ordered state. Anisotropy of the Mn^{2+} spins is small.¹⁹ Therefore, a gap of spin-wave excitations is small. We may observe spin-wave excitations in the vicinity of 0 meV in addition to the trimer excitations.

IV. SUMMARY

In order to confirm the spin system, we performed INS experiments of powders of the spin- $5/2$ antiferromagnetic trimer substance $\text{SrMn}_3\text{P}_4\text{O}_{14}$. We observed plural magnetic excitations. The peak positions are 0.46 , 0.68 , and 1.02 meV . The weak Q dependence of constant- Q scan spectra indicates that the excitations are transitions between discrete energy levels. The experimental results are consistent with results expected in the trimer model with the intratrimer interaction value of 0.29 meV (3.4 K) without considering the other interactions.

ACKNOWLEDGMENTS

We are grateful to T. Masuda for invaluable discussions. The neutron-scattering experiments were carried out in the framework of JAEA Users' Program and within the NIMS-RIKEN-JAEA Cooperative Research Program on Quantum Beam Science and Technology. This work was partially supported by grants from NIMS.

*HASE.Masashi@nims.go.jp

¹H. Nojiri, Y. Tokunaga, and M. Motokawa, *J. Phys. (Paris)* **49**, 1459 (1988).

²T. Nikuni and H. Shiba, *J. Phys. Soc. Jpn.* **62**, 3268 (1993).

³M. Hase, I. Terasaki, and K. Uchinokura, *Phys. Rev. Lett.* **70**, 3651 (1993).

⁴M. Hase, I. Terasaki, K. Uchinokura, M. Tokunaga, N. Miura, and H. Obara, *Phys. Rev. B* **48**, 9616 (1993).

⁵E. Dagotto, J. Riera, and D. Scalapino, *Phys. Rev. B* **45**, R5744 (1992).

⁶M. Azuma, Z. Hiroi, M. Takano, K. Ishida, and Y. Kitaoka, *Phys. Rev. Lett.* **73**, 3463 (1994).

⁷M. Hase, I. Terasaki, Y. Sasago, K. Uchinokura, and H. Obara, *Phys. Rev. Lett.* **71**, 4059 (1993).

⁸M. Hase, N. Koide, K. Manabe, Y. Sasago, K. Uchinokura, and A. Sawa, *Phys. B* **215**, 164 (1995).

⁹M. Hase, K. Uchinokura, R. J. Birgeneau, K. Hirota, and G. Shirane, *J. Phys. Soc. Jpn.* **65**, 1392 (1996).

¹⁰M. Azuma, Y. Fujishiro, M. Takano, M. Nohara, and H. Takagi, *Phys. Rev. B* **55**, R8658 (1997).

¹¹M. Azuma, M. Takano, and R. S. Eccleston, *J. Phys. Soc. Jpn.* **67**, 740 (1998).

¹²M. C. Martin, M. Hase, K. Hirota, G. Shirane, Y. Sasago, N. Koide, and K. Uchinokura, *Phys. Rev. B* **56**, 3173 (1997).

¹³M. Hase, M. Kohno, H. Kitazawa, O. Suzuki, K. Ozawa, G. Kido, M. Imai, and X. Hu, *Phys. Rev. B* **72**, 172412 (2005).

¹⁴M. Hase, A. Dönni, V. Yu. Pomjakushin, L. Keller, F. Gozzo, A. Cervellino, and M. Kohno, *Phys. Rev. B* **80**, 104405 (2009).

- ¹⁵L. Thomas, F. Lioni, R. Ballou, D. Gatteschi, R. Sessoli, and B. Barbara, *Nature (London)* **383**, 145 (1996).
- ¹⁶J. M. Hernandez, X. X. Zhang, F. Luis, J. Bartolome, J. Tejada, and R. Ziolo, *Europhys. Lett.* **35**, 301 (1996).
- ¹⁷J. M. Hernandez, X. X. Zhang, F. Luis, J. Tejada, J. R. Friedman, M. P. Sarachik, and R. Ziolo, *Phys. Rev. B* **55**, 5858 (1997).
- ¹⁸T. Yang, Y. Zhang, S. Yang, G. Li, M. Xiong, F. Liao, and J. Lin, *Inorg. Chem.* **47**, 2562 (2008).
- ¹⁹M. Hase, T. Yang, R. Cong, J. Lin, A. Matsuo, K. Kindo, K. Ozawa, and H. Kitazawa, *Phys. Rev. B* **80**, 054402 (2009).
- ²⁰A. Zheludev, G. Shirane, Y. Sasago, M. Hase, and K. Uchinokura, *Phys. Rev. B* **53**, 11642 (1996).
- ²¹M. Hase, M. Matsuda, K. Kakurai, K. Ozawa, H. Kitazawa, N. Tsujii, A. Dönni, M. Kohno, and X. Hu, *Phys. Rev. B* **76**, 064431 (2007).
- ²²M. Hase, M. Matsuda, K. Kakurai, K. Ozawa, H. Kitazawa, N. Tsujii, A. Dönni, and H. Kuroe, *Phys. Rev. B* **76**, 134403 (2007).
- ²³A. Furrer and H. U. Güdel, *J. Magn. Magn. Mater.* **14**, 256 (1979).
- ²⁴M. Matsuda, K. Kakurai, A. A. Belik, M. Azuma, M. Takano, and M. Fujita, *Phys. Rev. B* **71**, 144411 (2005).
- ²⁵A. Podlesnyak, V. Y. Pomjakushin, E. V. Pomjakushina, K. Conder, and A. Furrer, *Phys. Rev. B* **76**, 064420 (2007).
- ²⁶P. J. Brown, *International Tables for Crystallography*, edited by E. Prince (International Union of Crystallography, Chester, 2006), Vol. C, Chap. 4.4.5, p. 454.
- ²⁷B. Leuenberger, A. Stebler, H. U. Güdel, A. Furrer, R. Feile, and J. K. Kjems, *Phys. Rev. B* **30**, 6300 (1984).
- ²⁸P. S. Häfliger, S. T. Ochsenbein, B. Trusch, H. U. Güdel, and A. Furrer, *J. Phys. Condens. Matter* **21**, 026019 (2009).
- ²⁹Y. Sasago, K. Uchinokura, and A. Zheludev, and G. Shirane, *Phys. Rev. B* **55**, 8357 (1997).
- ³⁰M. Hase, V. Yu. Pomjakushin, L. Keller, A. Dönni, O. Sakai, T. Yang, R. Cong, J. Lin, K. Ozawa, and H. Kitazawa, e-print arXiv:1111.1782 [cond-mat], *Phys. Rev. B* (to be published).